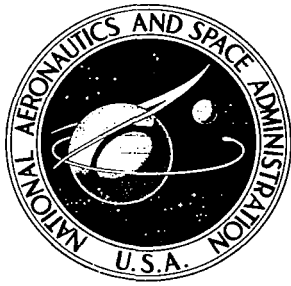


NASA CR-1155

NASA CONTRACTOR  
REPORT



TLE0371



TECH LIBRARY KAFB, NM

NASA CONTRACTOR

REPORT

LOAN COPY: RETURN TO  
AFWL (WLIL-2)  
KIRTLAND AFB, N.MEX

# NOISE REDUCTION SHAPE FACTORS IN THE LOW-FREQUENCY RANGE

*by J. Ronald Bailey and Franklin D. Hart*

*Prepared by*

**NORTH CAROLINA STATE UNIVERSITY**

Raleigh, N. C.

*for*

**NATIONAL AERONAUTICS AND SPACE ADMINISTRATION • WASHINGTON, D. C. • SEPTEMBER 1968**

NASA CR-1155  
TECH LIBRARY KAFB, NM



NOISE REDUCTION SHAPE FACTORS  
IN THE LOW-FREQUENCY RANGE

By J. Ronald Bailey and Franklin D. Hart

Distribution of this report is provided in the interest of information exchange. Responsibility for the contents resides in the author or organization that prepared it.

Prepared under Grant No. NGR-34-002-035 by  
NORTH CAROLINA STATE UNIVERSITY  
Raleigh, N.C.

for

NATIONAL AERONAUTICS AND SPACE ADMINISTRATION

---

For sale by the Clearinghouse for Federal Scientific and Technical Information  
Springfield, Virginia 22151 - CFSTI price \$3.00



## TABLE OF CONTENTS

	Page
LIST OF FIGURES . . . . .	iv
INTRODUCTION . . . . .	1
REVIEW OF LITERATURE . . . . .	3
THEORETICAL DEVELOPMENT . . . . .	9
Rectangular Panel . . . . .	9
Circular Panel . . . . .	11
Cylindrical Shell . . . . .	12
Spherical Shell . . . . .	15
Noise Reduction Design Charts . . . . .	15
EXPERIMENTAL INVESTIGATION . . . . .	33
SUMMARY AND CONCLUSIONS . . . . .	42
LIST OF REFERENCES . . . . .	44
APPENDIX. LIST OF SYMBOLS . . . . .	45

## LIST OF FIGURES

	Page
1. Arrangement for measuring NR . . . . .	4
2. Characteristic panel behavior . . . . .	6
3. Uniformly loaded rectangular flat plate . . . . .	10
4. Uniformly loaded circular flat plate . . . . .	10
5. Cylindrical shell . . . . .	16
6. Spherical shell . . . . .	16
7. Noise reduction with one supported steel panel . . . . .	17
8. Noise reduction with one clamped steel panel . . . . .	18
9. Noise reduction with one supported steel panel . . . . .	19
10. Noise reduction with one clamped steel panel . . . . .	20
11. Noise reduction with one supported aluminum panel . . . . .	21
12. Noise reduction with one clamped aluminum panel . . . . .	22
13. Noise reduction with one supported aluminum panel . . . . .	23
14. Noise reduction with one clamped aluminum panel . . . . .	24
15. Noise reduction with one supported circular steel panel . . . . .	26
16. Noise reduction with one clamped circular steel panel . . . . .	27
17. Noise reduction with one supported circular aluminum panel . . . . .	28
18. Noise reduction with one clamped circular aluminum panel . . . . .	29
19. Noise reduction with cylindrical panels . . . . .	31
20. Noise reduction of spherical enclosures . . . . .	32
21. Experimental arrangement . . . . .	34
22. Arrangement of instrumentation . . . . .	35
23. Sound model . . . . .	36
24. Experimental noise reduction . . . . .	36

LIST OF FIGURES (continued)

	Page
25. Experimental noise reduction . . . . .	38
26. Sound model . . . . .	39
27. Experimental noise reduction . . . . .	39
28. Sound model . . . . .	41
29. Experimental noise reduction . . . . .	41



## SUMMARY

An analysis is made of noise reduction of small enclosures in the low-frequency range where both panel and volume are stiffness controlled. The strong dependence on geometry of the compliance of flexible panels is illustrated. Shape factors for low-frequency noise reduction are established through expressions for the acoustic compliance of enclosures and the compliances of rectangular, circular, cylindrical, and spherical panels. A comparison is made of the noise reduction of enclosures involving these elements and having equal volume, panel thickness, and exposed surface area. It is observed that the stiffer, membrane-controlled spherical and cylindrical enclosures have greater noise reduction than enclosures having flexure-controlled flat panels. A companion experimental investigation is described and the results are discussed and compared with the theory.

## INTRODUCTION

The study of low-frequency noise reduction has become increasingly important with the advent of large energy conversion units such as the rocket engine which produces high levels of low-frequency sound. This increased interest is due to concern for the physiological and psychological effects of low-frequency sound on man and the desire to isolate small assemblies from acoustic excitation.

Noise reduction, which is essentially a measure of the sound-insulation effectiveness of an enclosure, is dependent upon acoustic properties of the enclosure as well as transmission properties of the enclosure walls. Classical noise reduction theory as presented in the literature (Beranek, 1960) has many applications in architecture. However, classical analysis applies only for panels whose dimensions are longer than a few acoustic wavelengths. Hence, classical analysis is invalid for many structures in the low-frequency range where the acoustic wavelengths are of the same order as the panel dimensions.

A general method for calculating low-frequency noise reduction has been presented in the literature (Lyon, 1963). Accordingly, when an external sound pressure  $P$  is applied to an enclosure, the initial volume  $V_b$  will decrease by an amount  $X$ . The resulting internal sound pressure will be given by

$$P_b = X/C_b , \quad (1)$$

where  $C_b$  is the acoustic compliance of the enclosure defined as

$$C_b = V_b/\rho C_a^2 , \quad (2)$$

$V_b$  = free volume of enclosure,

$\rho$  = density of air,

$C_a$  = speed of sound in air.

The volume displacement may also be written as

$$X = C_p (P - P_b) , \quad (3)$$

where  $C_p$  is the compliance of the enclosure walls. Noise reduction can thus be defined as a function of panel and volume compliances by the equation

$$NR \equiv 20 \log P/P_b \equiv 20 \log (1 + C_b/C_p) . \quad (4)$$

Since panel compliance is a strong function of geometry, the shape of a flexible panel exposed to a sound field can have a very significant effect on noise reduction. Thus, the purpose of this paper is to determine shape factors in low-frequency noise reduction. These shape factors are established through expressions for the compliances of rectangular, circular, cylindrical, and spherical panels and by comparison of the noise reduction of enclosures involving these elements and having equal volume, panel thickness, and exposed surface area. It is expected that the stiffer, membrane-controlled spherical and cylindrical enclosures will have greater noise reduction than enclosures having flat, flexure-controlled panels. A companion experimental investigation is described and the results are discussed and compared with the theory.

## REVIEW OF LITERATURE

The problem of determining the noise reduction of an enclosure has been handled in the past by a classical analysis which is usually defined in terms of an arrangement like that shown in Figure 1. It consists of two adjoining compartments or rooms separated by a panel of which noise reduction characteristics are in question.

The noise reduction of the separating panel has been defined (Beranek, 1960; Lyon et al., 1966) as

$$NR = 10 \log \left| \frac{P_1}{P_2} \right|^2 , \quad (5)$$

where  $P_1$  is the sound pressure level produced by a source in room 1 and  $P_2$  is the resulting sound pressure level in room 2. Noise reduction by this definition obviously depends on the absorption properties of the receiving room as well as the transmission properties of the separating panel.

Noise reduction has also been defined (Beranek, 1960; Lyon et al., 1966) as the reduction in sound pressure level resulting from the insertion of the panel between the previously unseparated rooms. The noise reduction contributed by the panel is usually defined as the transmission loss,

$$TL = 10 \log (\pi_{inc} / \pi_{trans}) , \quad (6)$$

where  $\pi_{inc}$  is the acoustic power incident on the panel from the source room side and  $\pi_{trans}$  is the power radiated into the receiving room.

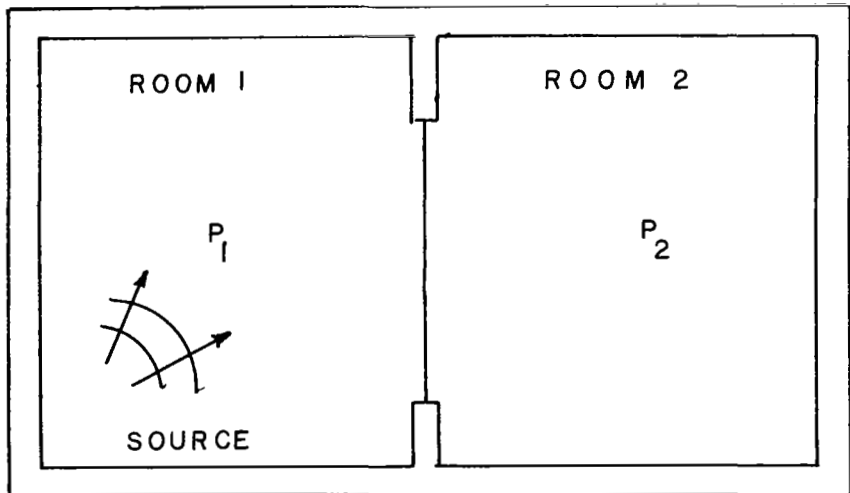


FIGURE 1. ARRANGEMENT FOR MEASURING NR

The behavior of a panel has been separated into three frequency regions (Beranek, 1960, p. 287) as shown in Figure 2. In Region I, below the lowest resonance frequency, mass and damping are unimportant as stiffness alone controls the behavior of the panel. Above the first few resonances in Region II the mass becomes most important. This mass-controlled region may extend from two or three times the lowest resonance frequency up to the critical frequency where the bending wavelength in the panel equals the acoustic wavelength in the surrounding medium.

Classical noise-reduction theory has many applications in architecture. However, classical noise reduction analysis applies only for panels whose dimensions are longer than a few acoustic wavelengths. Hence, these calculations are invalid for many structures in the low-frequency range where the acoustic wavelengths are of the same order as the panel dimensions.

Lyon (1963) computed the theoretical noise reduction of a rigid rectangular enclosure with one flexible wall. He considered noise reduction in three frequency ranges: (1) "low" frequencies where both panel and volume are stiffness controlled, (2) "intermediate" frequencies where the panel is resonant and the volume stiff, and (3) "high" frequencies where both panel and volume are resonant. Lyon also suggested that noise reduction of enclosures having more than one flexible panel can be calculated without difficulty if the motions of the various panels are properly correlated. For example, panels in the low-frequency would probably move in phase.

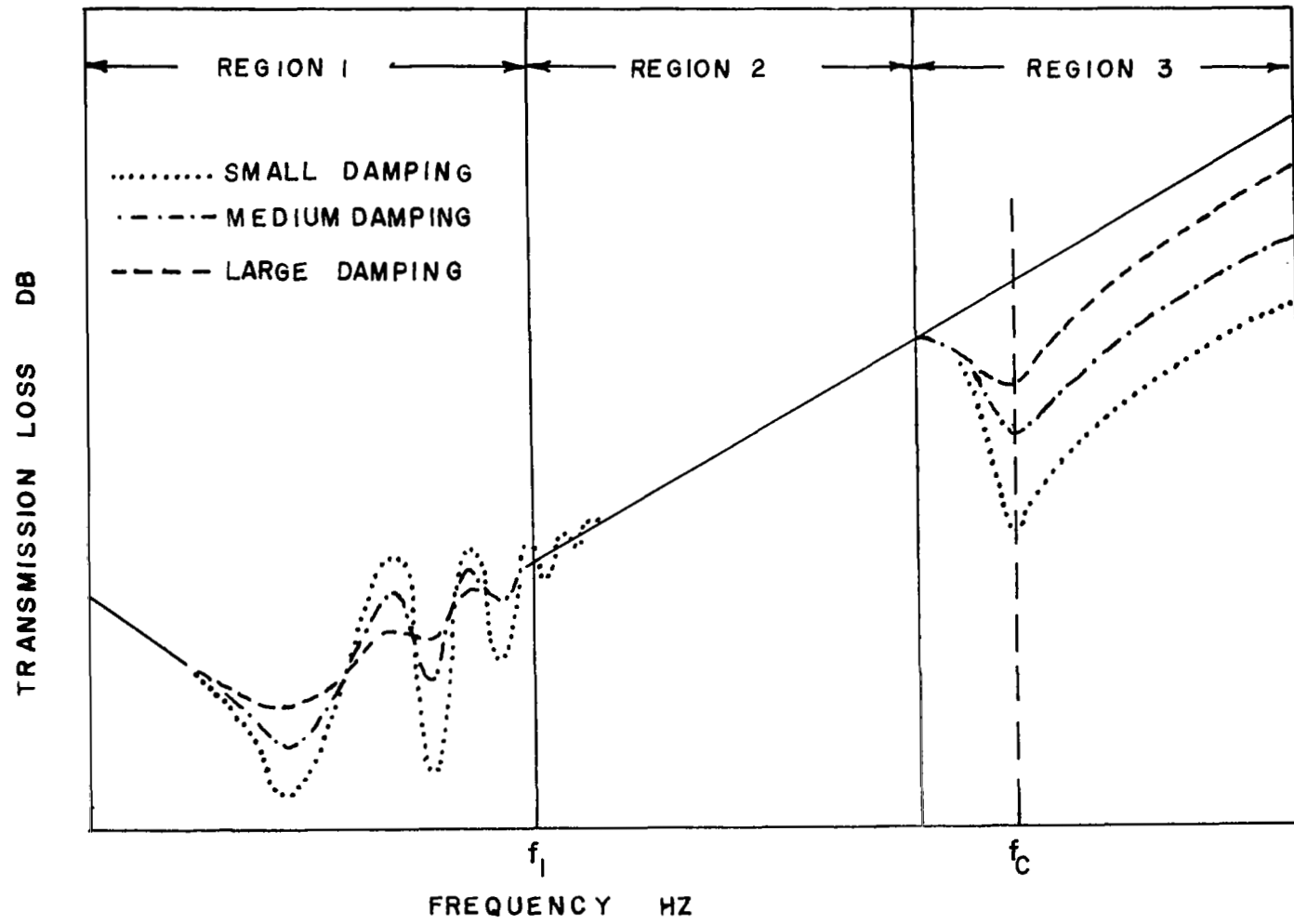


FIGURE 2. CHARACTERISTIC PANEL BEHAVIOR

Eichler (1965) presented a thermal circuit approach for calculating the noise reduction of a rectangular box. Assuming that the panels are attached to a rigid frame and hence mechanically isolated, he gave the following equation for the low-frequency noise reduction of the box,

$$NR = 10 \log \left( 1 + \frac{V}{\rho C^2} / \sum C_j \right)^2 \quad (7)$$

where the  $C_j$ 's are the compliances of the panels defined as volume displacements divided by pressure differences. This equation and the assumption of panel isolation are verified by experimental results which agree well with the theory.

Eichler also gave an expression for the noise reduction of a spherical enclosure as

$$NR = 10 \log \left( 1 + 2h C_w^2 \rho_w / 3C^2 \rho R \right)^2 , \quad (8)$$

where  $h$  = panel thickness,

$R$  = radius,

$\rho_w$  = panel density,

$\rho$  = density of air,

$C_w$  = speed of sound in panel,

$C$  = speed of sound in air.

An examination of equations (7) and (8) would indicate that the noise reduction of a rectangular box is much less than that of a spherical enclosure having the same material, weight, and enclosed volume.

White and Powell (1966) investigated sound transmission through a rectangular double wall from a statistical viewpoint. White (1966) also studied sound transmission through a finite, closed, cylindrical shell. However, he did not consider the low-frequency region.

Perhaps the most significant recent study of low-frequency noise reduction is that presented in a report by Lyon (1966) in which applications in spacecraft structures are considered. In this report, a review is made of the classical theory and a discussion is given of the inadequacies of this theory in the very low-frequency range and of the modifications that must be imposed in order to adequately express low-frequency noise reduction in analytical form.

## THEORETICAL DEVELOPMENT

In this section expressions are developed for the compliance of rectangular, circular, cylindrical and spherical panels. Equation (4) is then used to calculate the noise reduction of enclosures having these elements. The results are presented as design charts.

### Rectangular Panel

The compliance of a rectangular panel can be calculated by considering the uniformly loaded flat plate shown in Figure 3. The deflections for simply-supported and clamped edges are given by Love (1944) as

$$w_s = \frac{1}{64} \frac{P}{D} (x^2 + y^2) (x^2 + y^2 - \frac{2t^2}{1-\sigma}) , \quad (9)$$

and

$$w_c = \frac{P (a^2 - x^2)^2 (b^2 - y^2)^2}{24D (a^4 + b^4)} , \quad (10)$$

where  $P$  = pressure

$t$  = thickness

$2a$  = width

$2b$  = length

$\sigma$  = Poisson's ratio

$$D = \frac{Et^3}{12 (1 - \sigma^2)} .$$

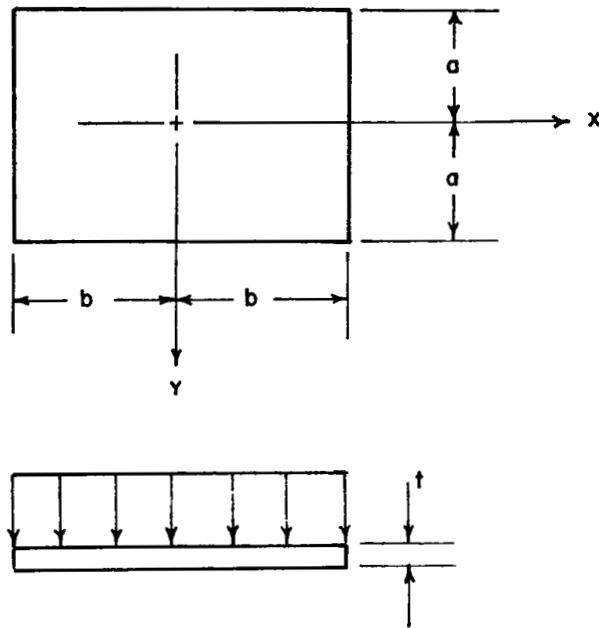


FIGURE 3. UNIFORMLY LOADED RECTANGULAR FLAT PLATE

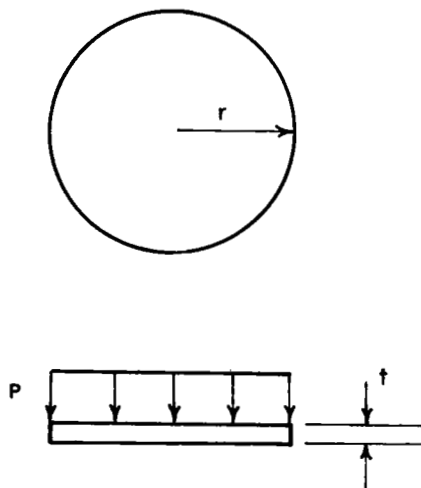


FIGURE 4. UNIFORMLY LOADED CIRCULAR FLAT PLATE

In general, the volume displacement is found by integrating over the area,

$$X = \int_{-a}^a \int_{-b}^b w(x,y) dx dy . \quad (11)$$

By integration and substitution, the compliances can be written

$$C_{P_s} = \frac{9a^5 b + 10a^3 b^3 + 9ab^5 - \frac{30t^2}{1-\sigma} (a^3 b + ab^3)}{1080 D} , \quad (12)$$

and

$$C_{P_c} = \frac{32 a^5 b^5}{675 D (a^4 + b^4)} . \quad (13)$$

### Circular Panel

The deflections of the circular plate shown in Figure 4 for simply-supported and clamped edges are given by Timoshenko (1959) as

$$w_s(r) = \frac{P(a^2 - r^2)}{64 D} \left( \frac{5 + \sigma}{1 + \sigma} a^2 - r^2 \right) , \quad (14)$$

and

$$w_c(r) = \frac{P}{64 D} (a^2 - r^2)^2 . \quad (15)$$

Volume displacement is again obtained by integrating over the area,

$$X = 2\pi \int_0^a w(r) r dr . \quad (16)$$

Integration and substitution yield the following expressions for the compliances of simply-supported and clamped circular plates

$$C_{P_s} = \frac{\pi a^6}{192 D} \frac{(7 + \sigma)}{(1 + \sigma)} , \quad (17)$$

and

$$C_{P_c} = \frac{\pi a^6}{192 D} . \quad (18)$$

### Cylindrical Shell

Now consider the cylinder shown in Figure 5. The radial deflection of a cylinder of radius  $a$  and thickness  $t$  subjected to internal pressure  $P$  is given by Timoshenko (1959) as

$$w(x) = \frac{Pa^2}{Et} - K_1 \sin \beta x \operatorname{Sinh} \beta x - K_2 \cos \beta x \operatorname{Cosh} \beta x, \quad (19)$$

where

$$\beta^4 = \frac{Et}{4a^2 D} .$$

For simply-supported ends the boundary conditions are

$$w(\ell/2) = 0$$

and

$$\frac{d^2 w}{dx^2} (\ell/2) = 0 .$$

These give

$$K_1 = \frac{Pa^2}{Et} \frac{2 \sin \alpha \operatorname{Sinh} \alpha}{\cos 2\alpha + \operatorname{Cosh} 2\alpha} , \quad (20)$$

and

$$K_2 = \frac{Pa^2}{Et} \frac{2 \cos \alpha \operatorname{Cosh} \alpha}{\cos 2\alpha + \operatorname{Cosh} 2\alpha} , \quad (21)$$

where

$$\alpha = \frac{\beta l}{2} .$$

For fixed ends the boundary conditions are

$$w(l/2) = \frac{dw}{dx}(\frac{l}{2}) = 0 ,$$

which yield

$$K_1 = \frac{Pa^2}{Et} \frac{2 (\sin \alpha \operatorname{Cosh} \alpha - \cos \alpha \operatorname{Sinh} \alpha)}{\sin 2\alpha + \operatorname{Sinh} 2\alpha} \quad (22)$$

and

$$K_2 = \frac{Pa^2}{Et} \frac{2 (\sin \alpha \operatorname{Cosh} \alpha + \cos \alpha \operatorname{Sinh} \alpha)}{\sin 2\alpha + \operatorname{Sinh} 2\alpha} . \quad (23)$$

The volume displacement is given by

$$x = 2 \pi a \int_{-l/2}^{l/2} w(x) dx .$$

Integration gives

$$X = 2 \pi a \left[ \frac{Pa^2 \ell}{Et} - \frac{K_1}{\beta} \sin \alpha \cosh \alpha - \cos \alpha \sinh \alpha - \frac{K_2}{\beta} \sin \alpha \cosh \alpha + \cos \alpha \sinh \alpha \right]. \quad (24)$$

By substitution of equations (16), (17), (18) and (19) into equation (20) it can be shown that the compliance of simply-supported and clamped cylindrical enclosures will be

$$C_{P_s} = \frac{2\pi a^3 \ell}{Et} \left[ 1 - \frac{\sinh \beta l + \sin \beta l}{\beta l (\cosh \beta l + \cos \beta l)} \right], \quad (25)$$

and

$$C_{P_c} = \frac{2\pi a^3 \ell}{Et} \left[ 1 - \frac{2(\cosh \beta l - \cos \beta l)}{\beta l (\sinh \beta l + \sin \beta l)} \right]. \quad (26)$$

If  $\beta l > 3$ , as pointed out in the literature (Lyon et al., 1966), equations (25) and (26) reduce to

$$C_{P_s} = \frac{2\pi a^3 \ell}{Et} \left[ 1 - (\beta \ell)^{-1} \right], \quad (27)$$

and

$$C_{P_c} = \frac{2\pi a^3 \ell}{Et} \left[ 1 - 2(\beta \ell)^{-1} \right]. \quad (28)$$

### Spherical Shell

Consider the spherical segment of radius  $r$  and height  $h$  shown in Figure 6. If the shell is subjected to uniform pressure  $P$  the resulting deflection will be (Timoshenko, 1959)

$$W = \frac{Pr^2}{2 Et} (1 - \sigma) . \quad (29)$$

Volume displacement can be obtained by multiplying by the surface area.

$$X = W A = \frac{\pi Pr^3 L}{Et} (1 - \sigma) . \quad (30)$$

Thus the panel compliance may be written

$$C_p = \frac{\pi r^3 h}{Et} (1 - \sigma) . \quad (31)$$

### Noise Reduction Design Charts

Expressions have been derived for the compliance of rectangular, circular, cylindrical, and spherical panels. Design charts for the noise reduction of enclosures having these elements can now be presented by substituting into Equation (4).

The noise reduction of rectangular enclosures with a single flexible panel is plotted against the thickness ratio for three depth to width ratios in Figures 7 through 14.

Figures 7 and 8 give the noise reduction with a square steel panel having simply-supported and clamped edges. As can be seen in these figures, boundary conditions do not appreciably affect the noise reduction.

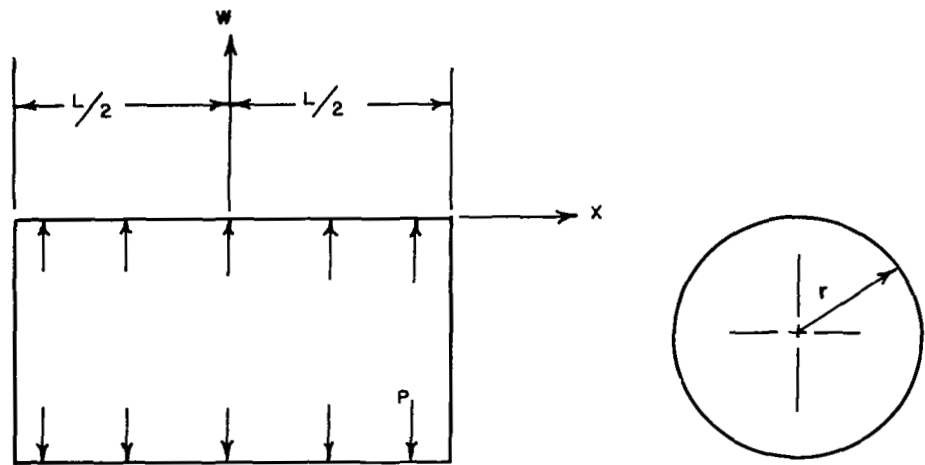


FIGURE 5. CYLINDRICAL SHELL

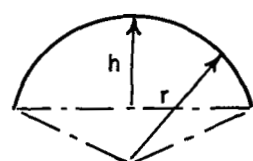


FIGURE 6. SPHERICAL SHELL

# **Error**

---

An error occurred while processing this page. See the system log for more details.

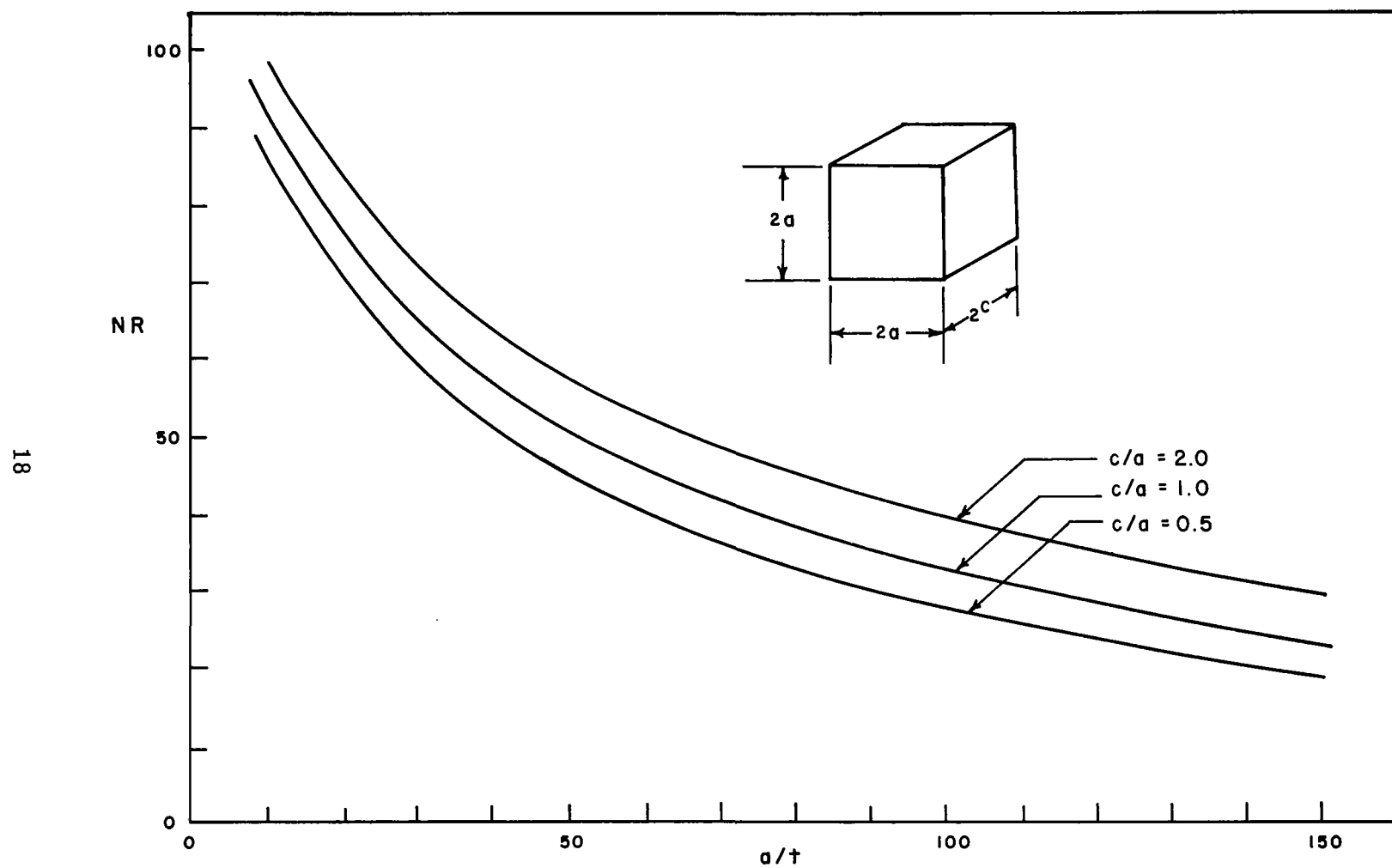


FIGURE 8. NOISE REDUCTION WITH ONE CLAMPED STEEL PANEL

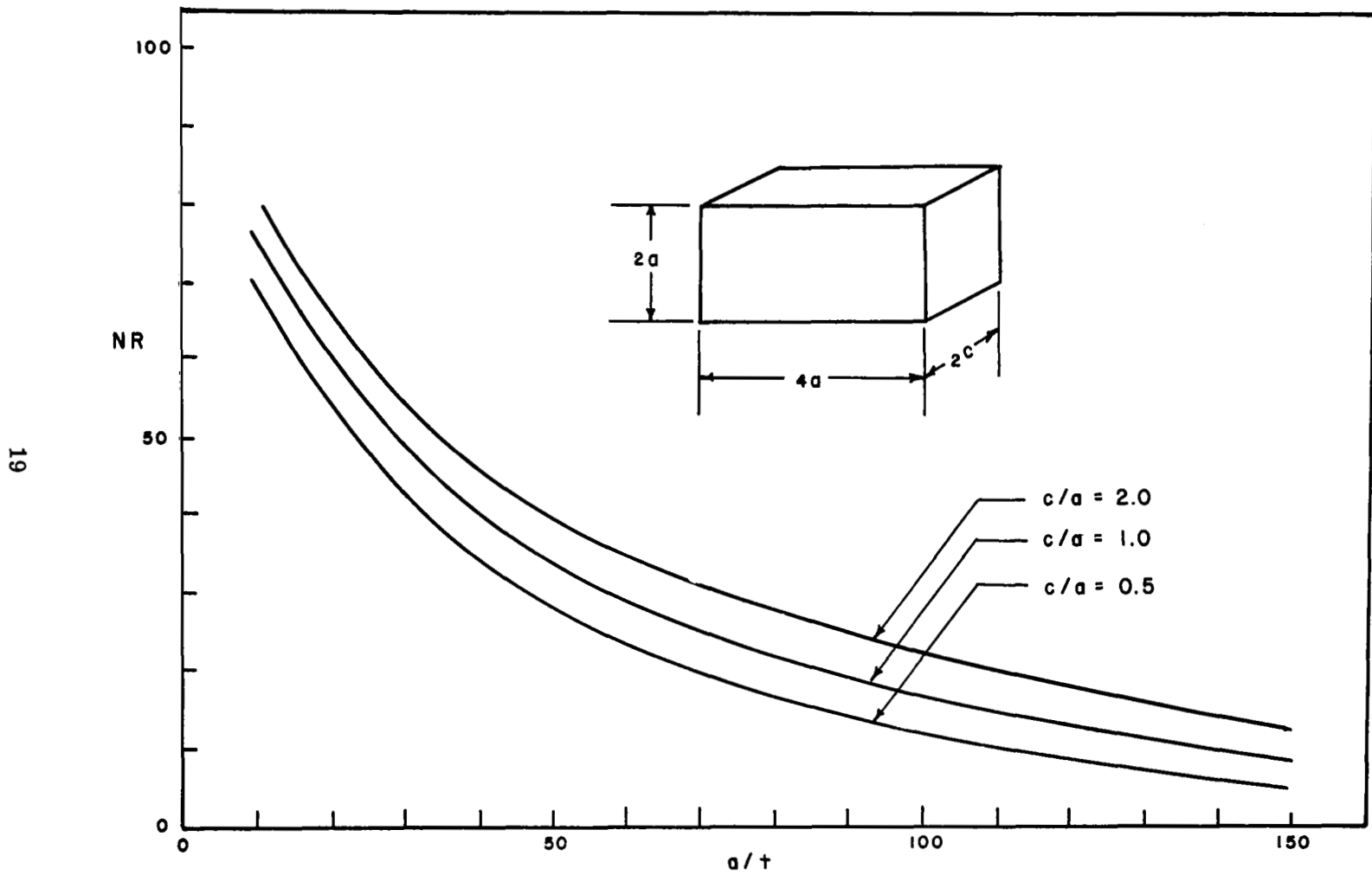


FIGURE 9. NOISE REDUCTION WITH ONE SUPPORTED STEEL PANEL

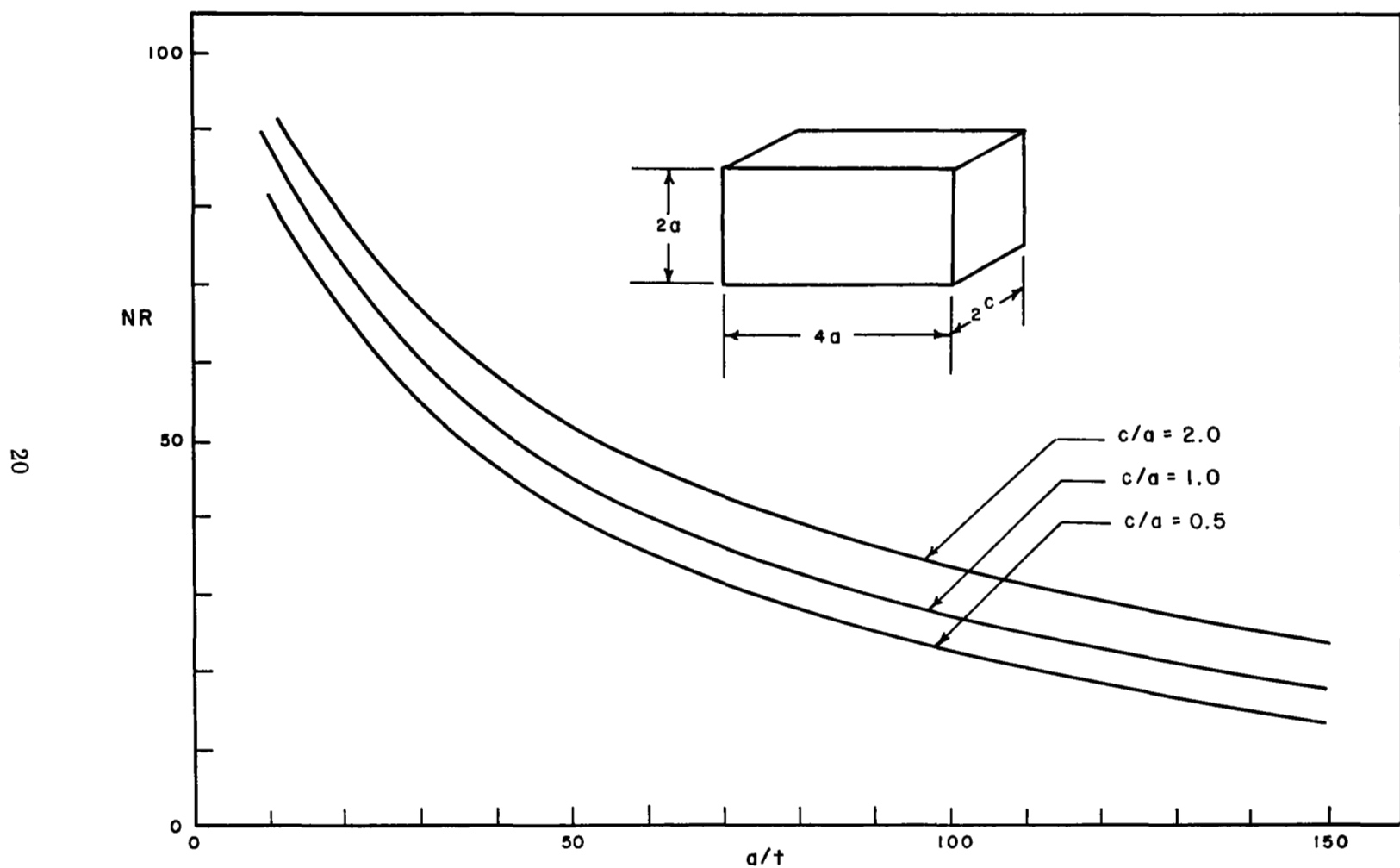


FIGURE 10. NOISE REDUCTION WITH ONE CLAMPED STEEL PANEL

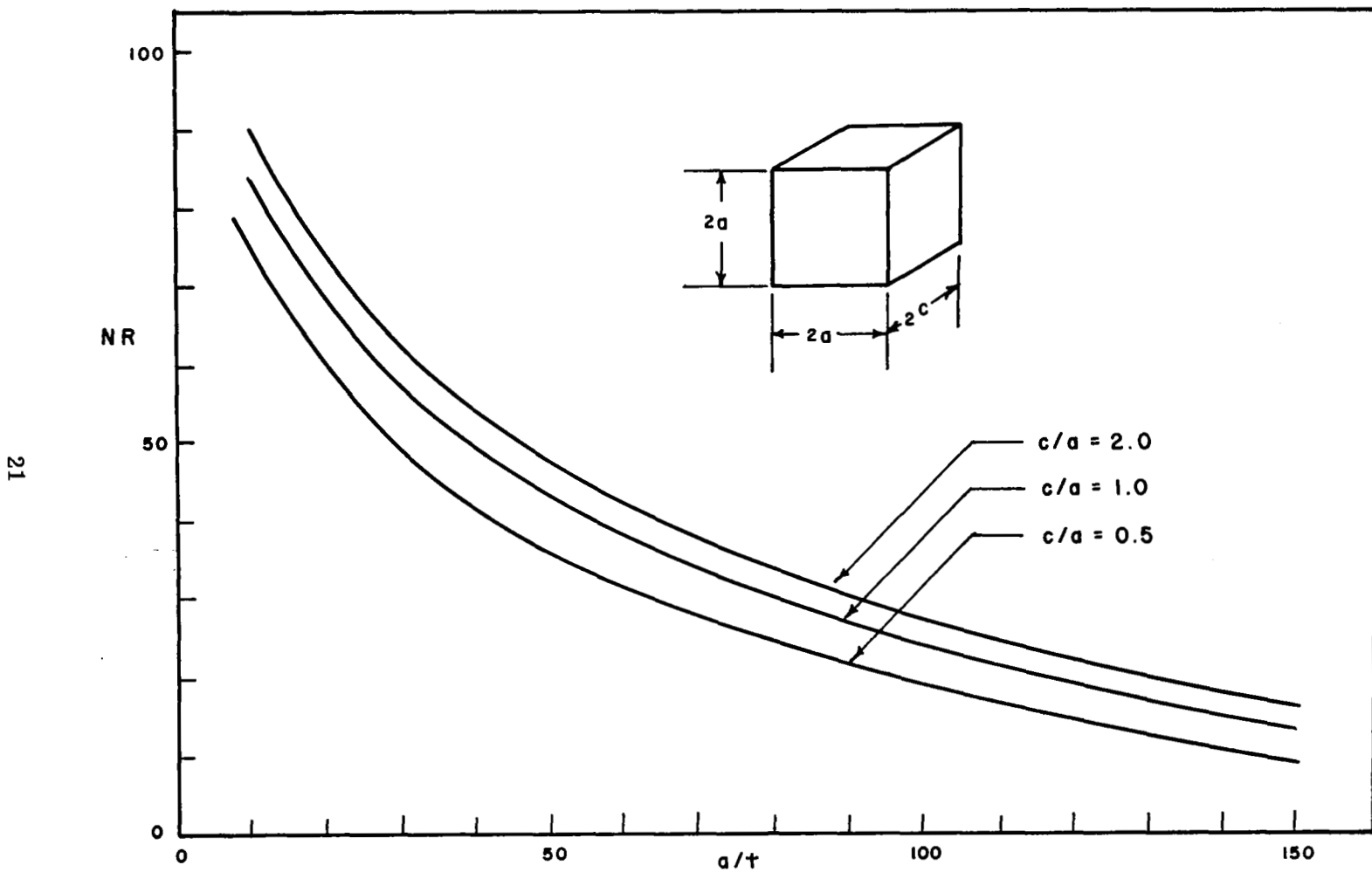


FIGURE II. NOISE REDUCTION WITH ONE SUPPORTED ALUMINUM PANEL

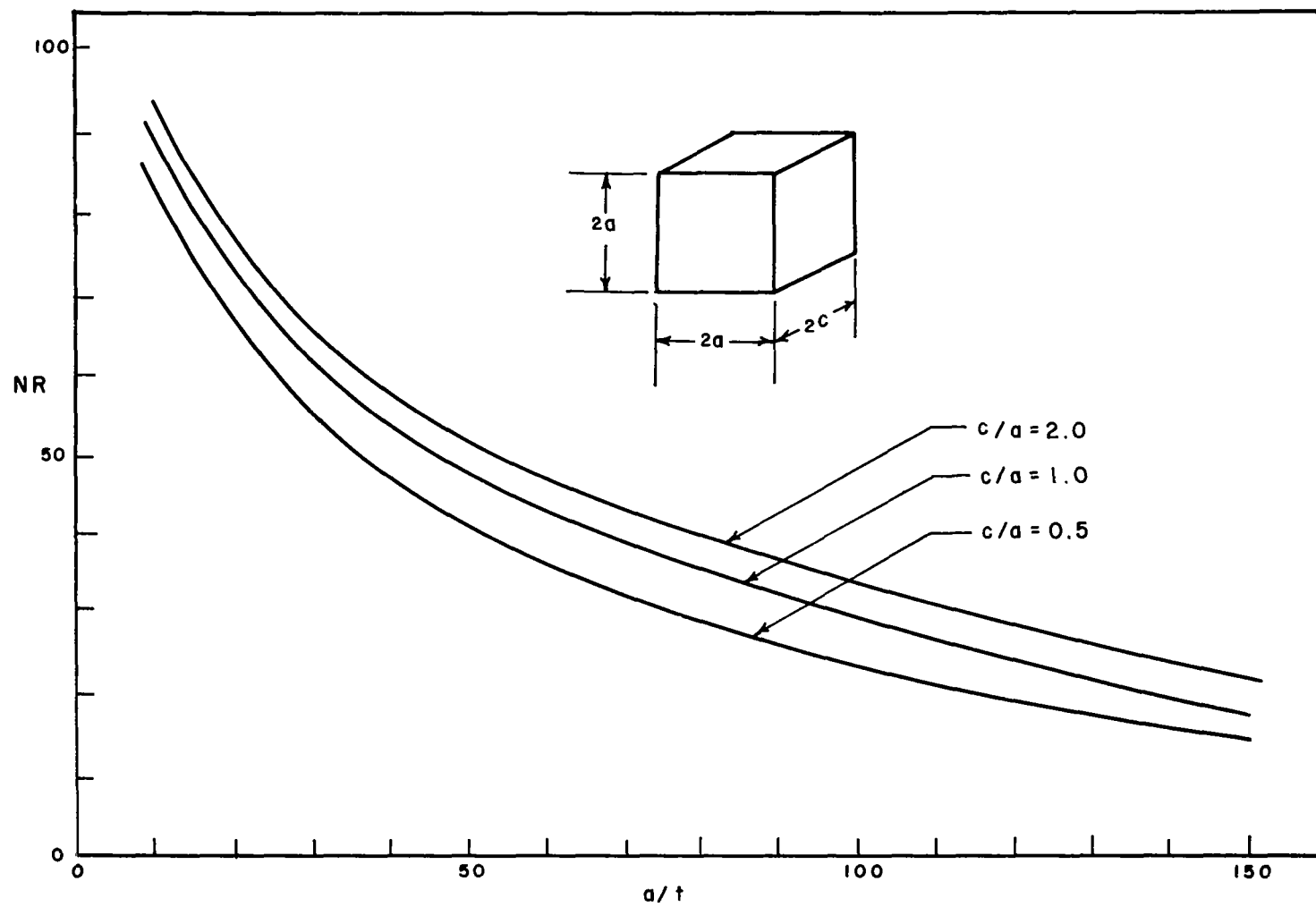


FIGURE 12. NOISE REDUCTION WITH ONE CLAMPED ALUMINUM PANEL

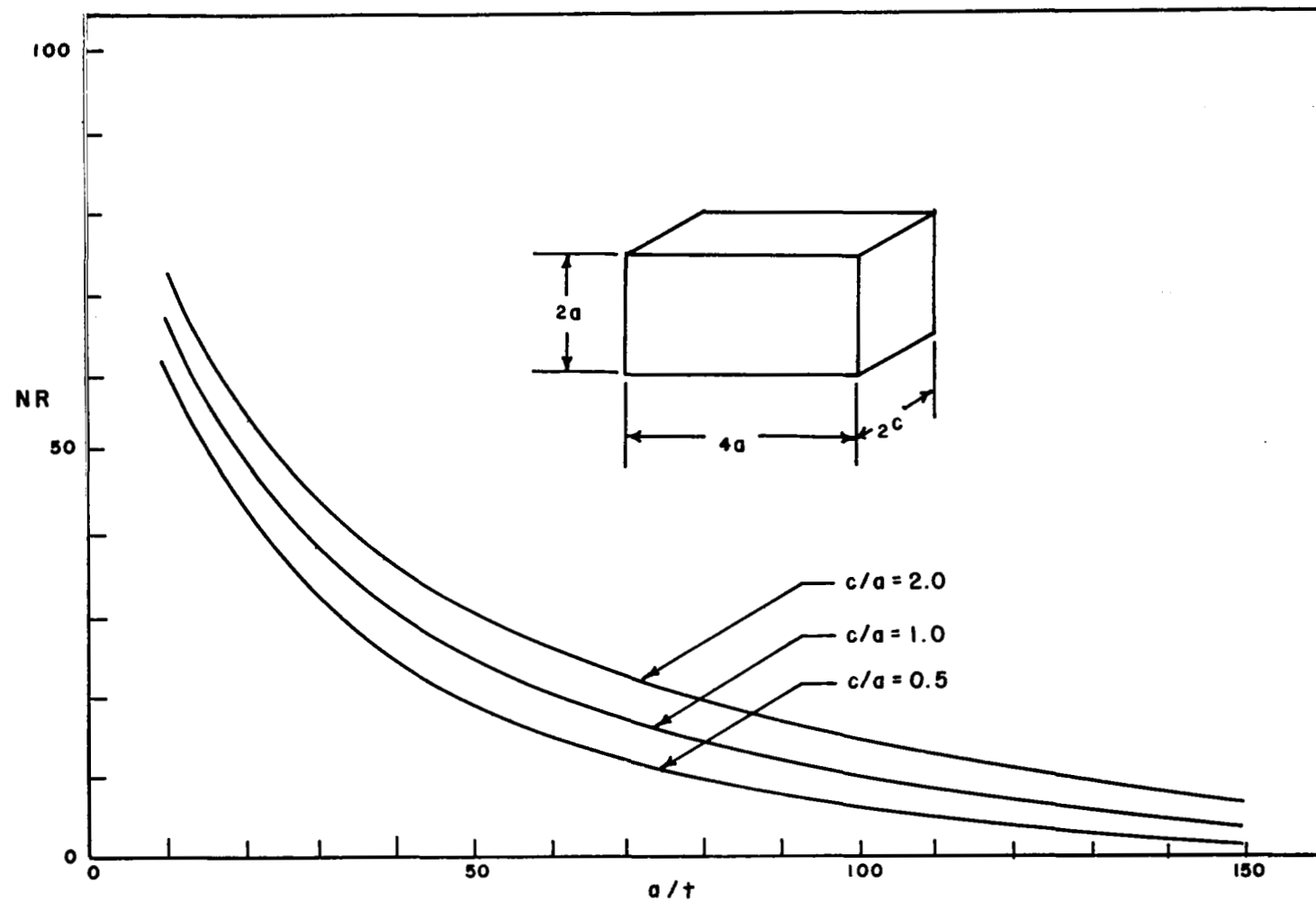


FIGURE 13. NOISE REDUCTION WITH ONE SUPPORTED ALUMINUM PANEL

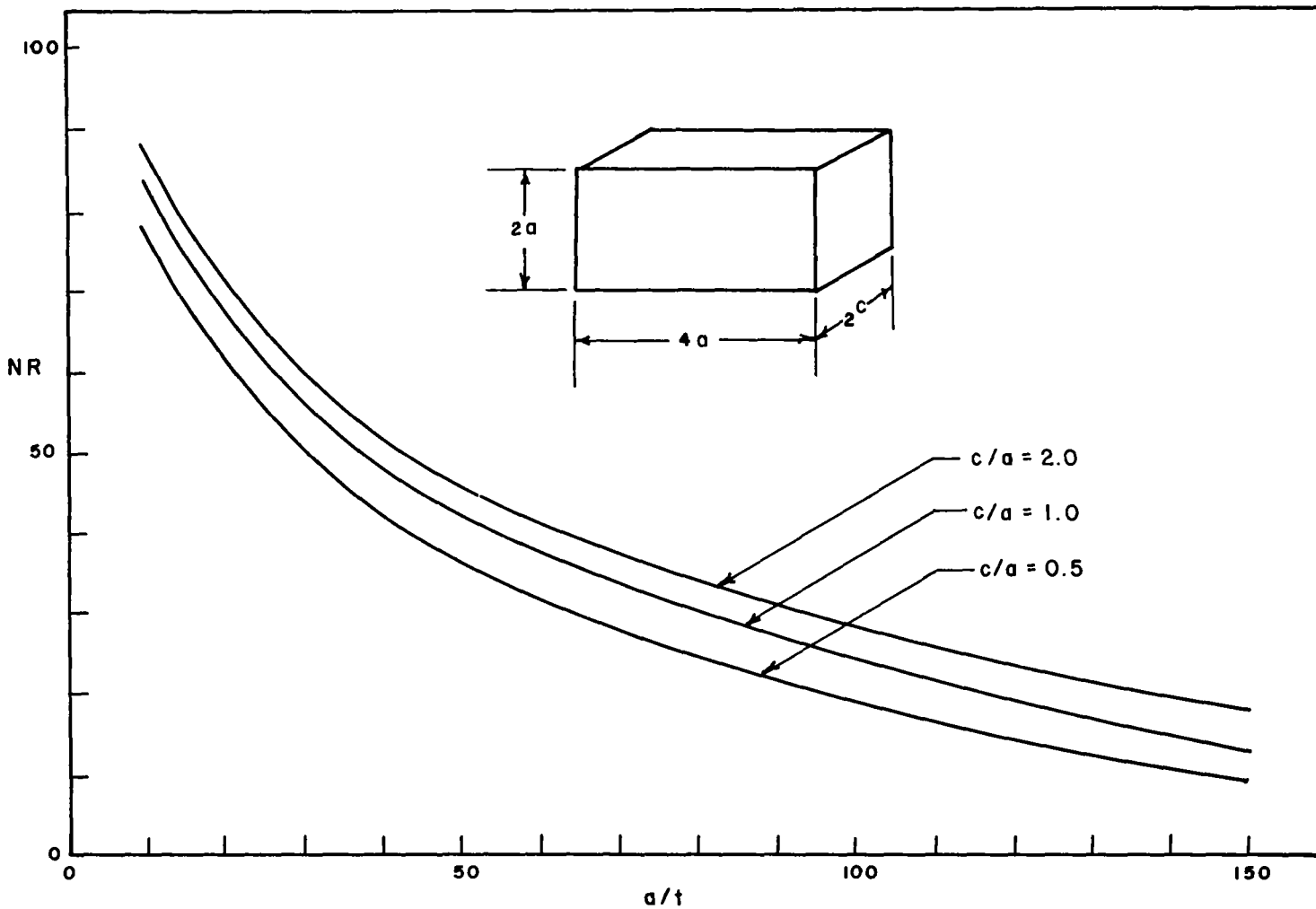


FIGURE 14. NOISE REDUCTION WITH ONE CLAMPED ALUMINUM PANEL

The noise reduction of enclosures with a single rectangular steel panel ( $b/a = 2$ ) having simply-supported and clamped edges is shown in Figures 9 and 10, respectively. In this case, clamped edges give approximately 10 dB greater reduction than supported edges for all depth ratios.

Figures 11 and 12 give the noise reduction of enclosures with a single square aluminum panel having simply-supported and clamped edges. It can be noted that clamped edges result in approximately 5 dB greater noise reduction. Also, comparison with Figures 7 and 8 show that steel panels have approximately 10 dB greater noise reduction than aluminum panels for all cases.

The noise reduction of enclosures with a single rectangular ( $b/a = 2$ ) aluminum panel having simply-supported and clamped edges is shown in Figures 13 and 14, respectively. Clamped edges yield approximately 15 dB greater noise reduction than supported edges and comparison with Figures 9 and 10 shows that steel panels have from 5 to 10 dB greater noise reduction than aluminum panels.

Figures 15 through 18 give the noise reduction of enclosures with steel and aluminum circular panels having simply-supported and clamped edges. It can be seen that panels with clamped edges have approximately 15 dB more noise reduction than those with supported edges and steel panels have approximately 10 dB greater noise reduction than aluminum panels. Also, increasing the volume by 5X increases noise reduction by about 15 dB in all cases.

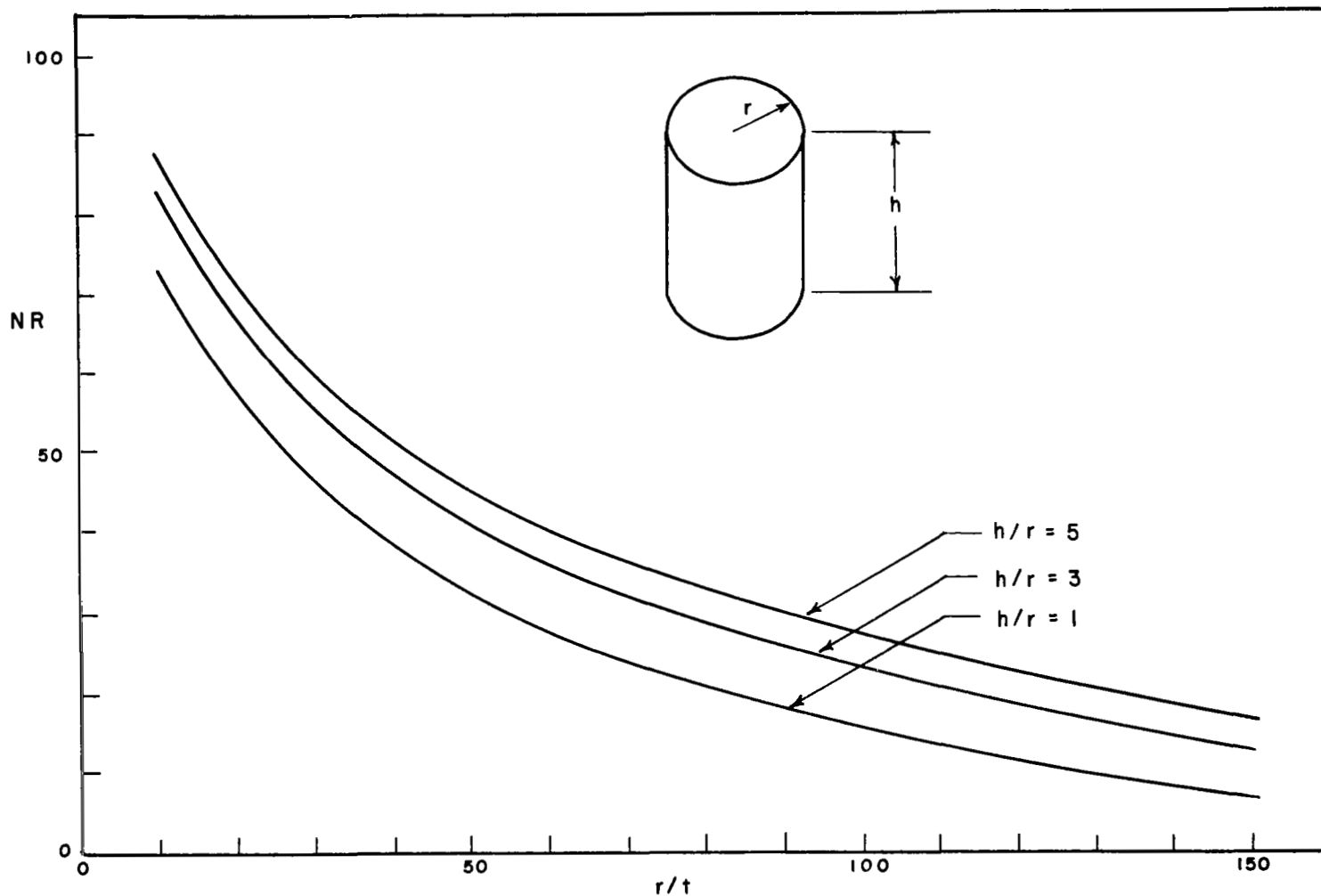


FIGURE 15. NOISE REDUCTION WITH ONE SUPPORTED CIRCULAR STEEL PANEL

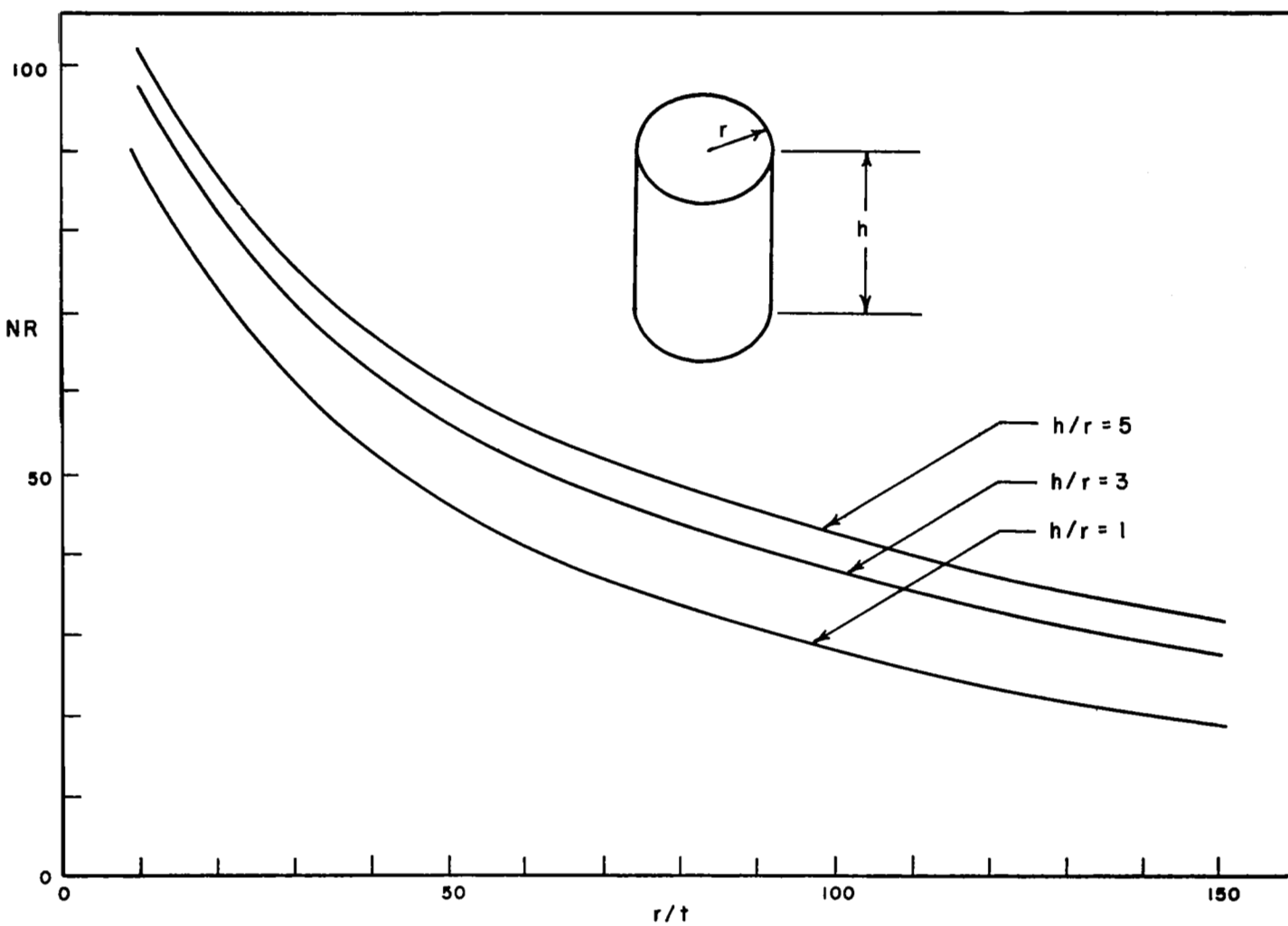


FIGURE 16. NOISE REDUCTION WITH ONE CLAMPED CIRCULAR STEEL PANEL

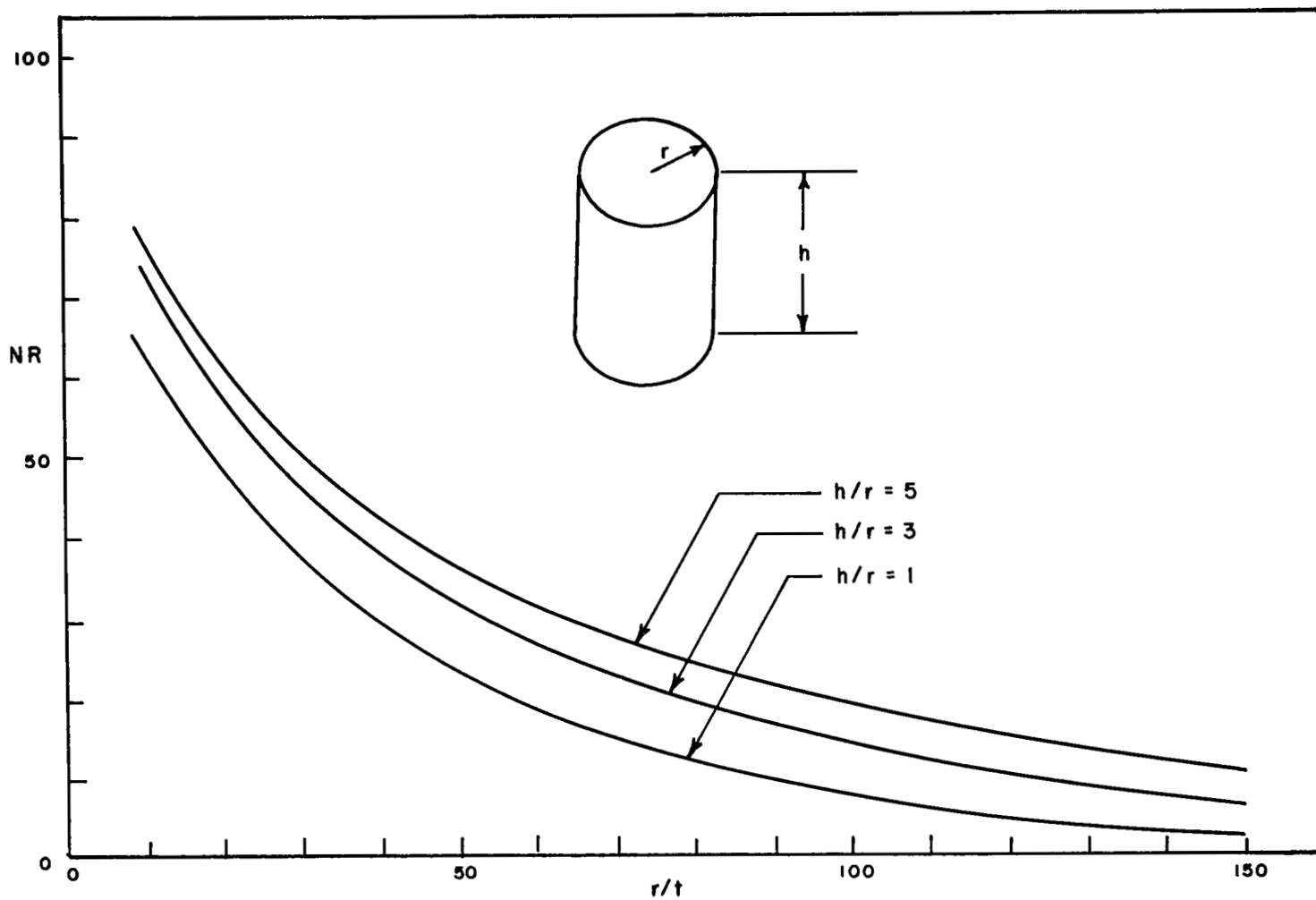


FIGURE 17. NOISE REDUCTION WITH ONE SUPPORTED CIRCULAR ALUMINUM PANEL

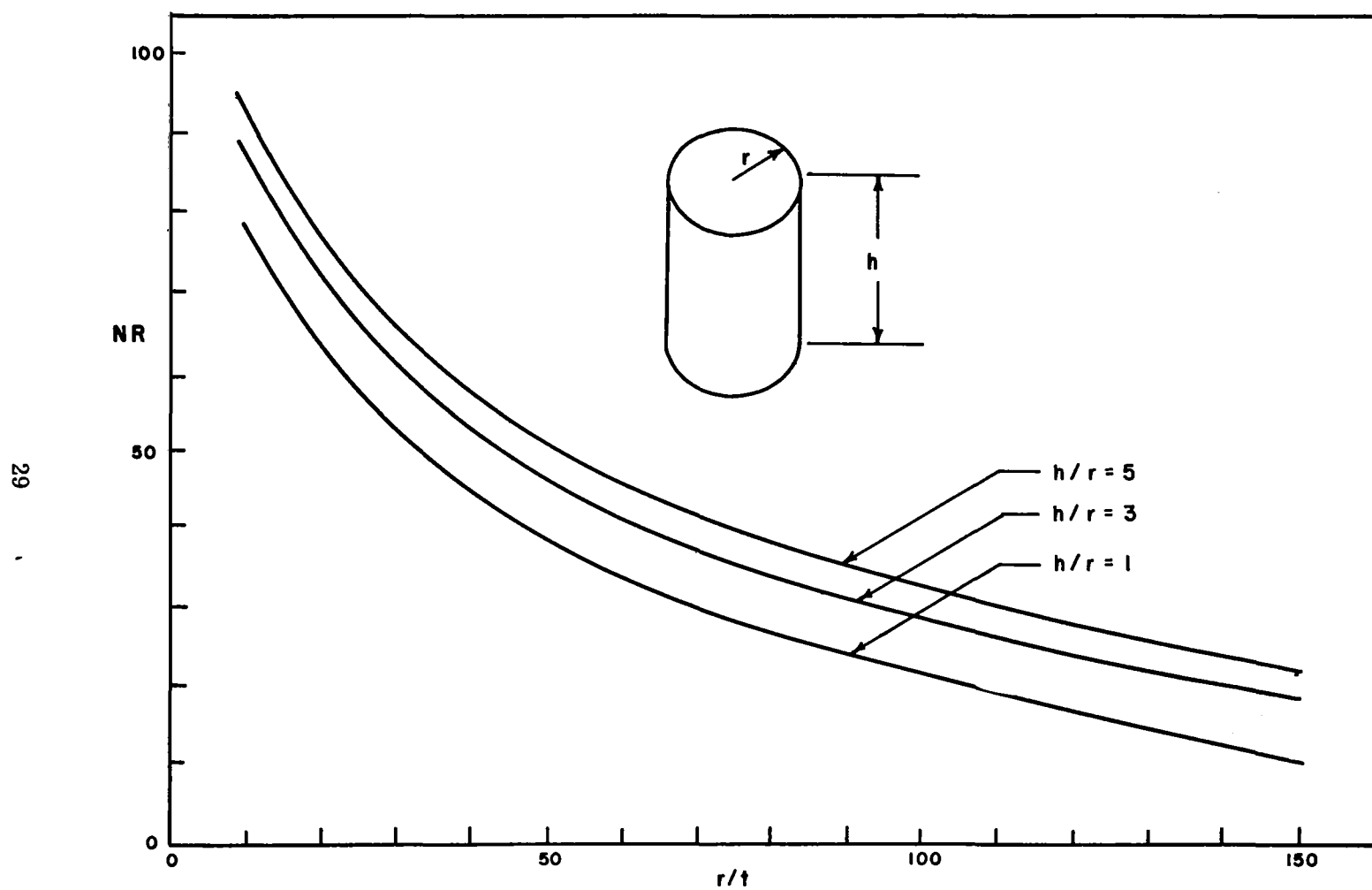


FIGURE 18. NOISE REDUCTION WITH ONE CLAMPED CIRCULAR ALUMINUM PANEL

The noise reduction of cylindrical enclosures with  $Bt > 20$  is shown in Figure 19. Steel panels again have about 10 dB greater noise reduction than aluminum panels and the slope of both curves is seen to be essentially constant for  $r/t > 100$ .

Figure 20 gives the noise reduction of steel and spherical enclosures. These curves are similar to those of Figures 19 in that steel panels have approximately 10 dB greater noise reduction than aluminum panels and the slope of the curves is essentially constant for  $r/t > 100$ .

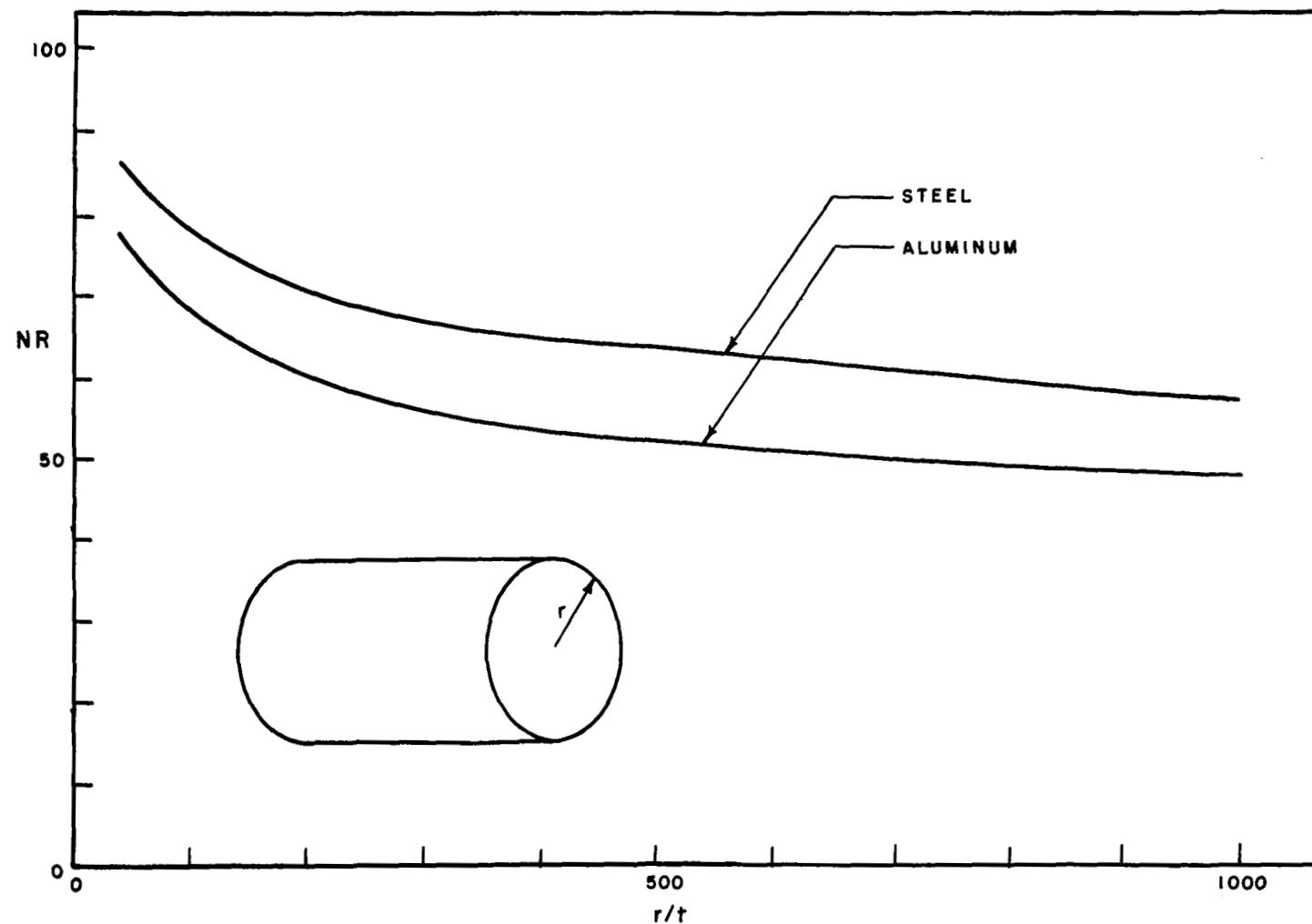


FIGURE 19. NOISE REDUCTION WITH CYLINDRICAL PANELS

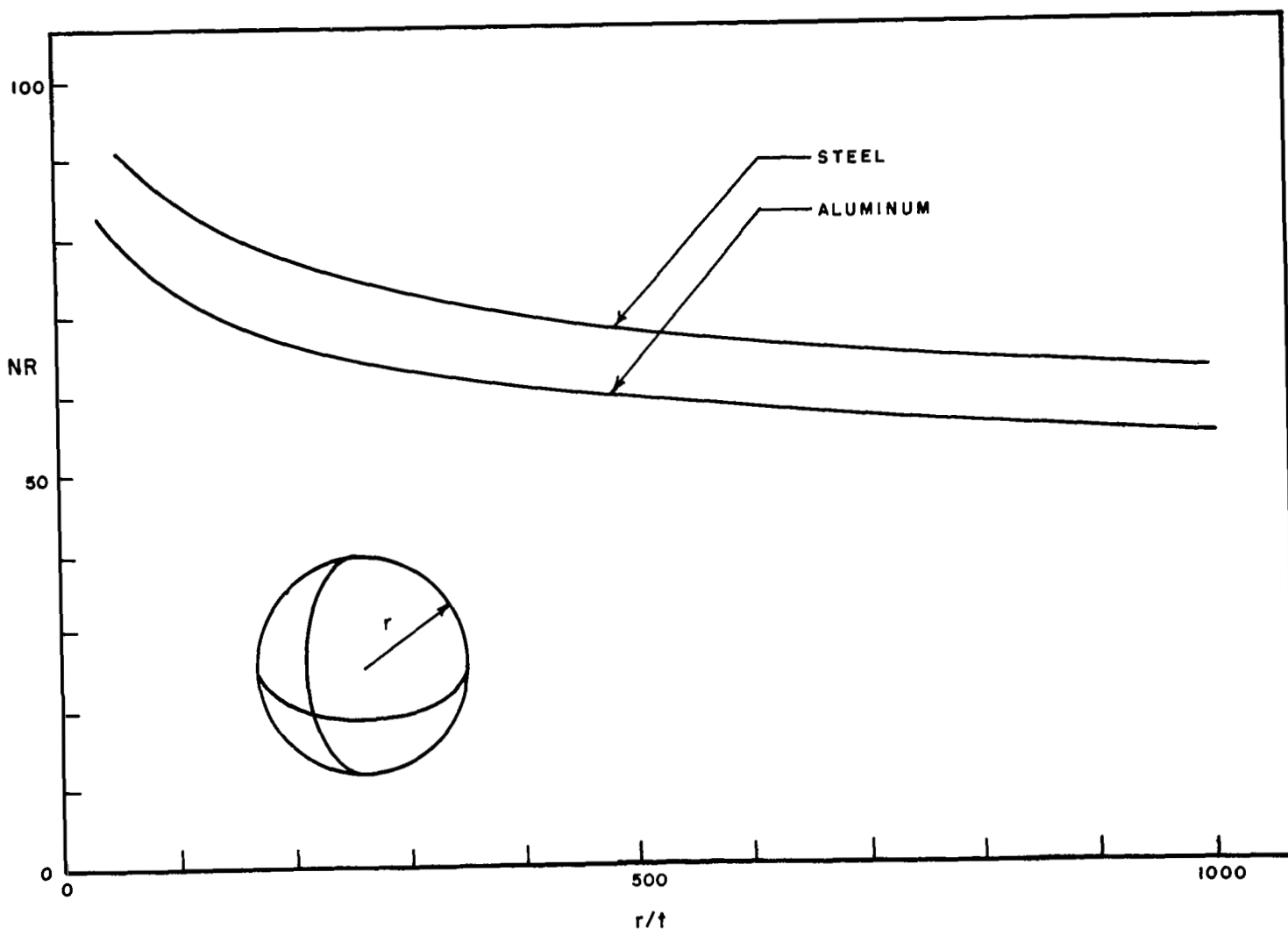


FIGURE 20. NOISE REDUCTION OF SPHERICAL ENCLOSURES

## EXPERIMENTAL INVESTIGATION

In this section, the experimental investigation is described and the results are discussed and compared with the theory. The objective of this study was to measure the noise reduction of enclosures having flat, cylindrical, and spherical walls.

The arrangement of the instrumentation used in this study is shown in Figure 21. It consists of an oscillator with a continuous sweep range of twenty to twenty thousand Hz. The signal from the oscillator was fed to a power amplifier and then to a loud speaker which was mounted on a plywood test chamber. The sound model with a pick-up microphone inside was suspended in the test chamber and the output of this microphone was fed through a signal amplifier to a graphic level recorder. A compressor microphone was also suspended in the test chamber and its signal fed back through an amplifier to the oscillator. In this way the sound pressure level inside the test chamber was kept constant over the desired frequency range. A photograph of the instrumentation is shown in Figure 22.

A water bath was used to test for small air leaks, and wax was used to seal the microphone in place. The microphones were calibrated with a Brueel and Kjaer pistonphone. Also, both microphones were placed in the sound enclosure without the model and the difference in the two recorded levels was set to zero. This was repeated for each test.

A photograph of the first enclosure is shown in Figure 23. It consists of a rectangular enclosure  $14\frac{1}{2}$  in. x  $14\frac{1}{2}$  in. x 2 in. with the back and sides made of  $\frac{1}{2}$  in. thickness aluminum. A test panel of

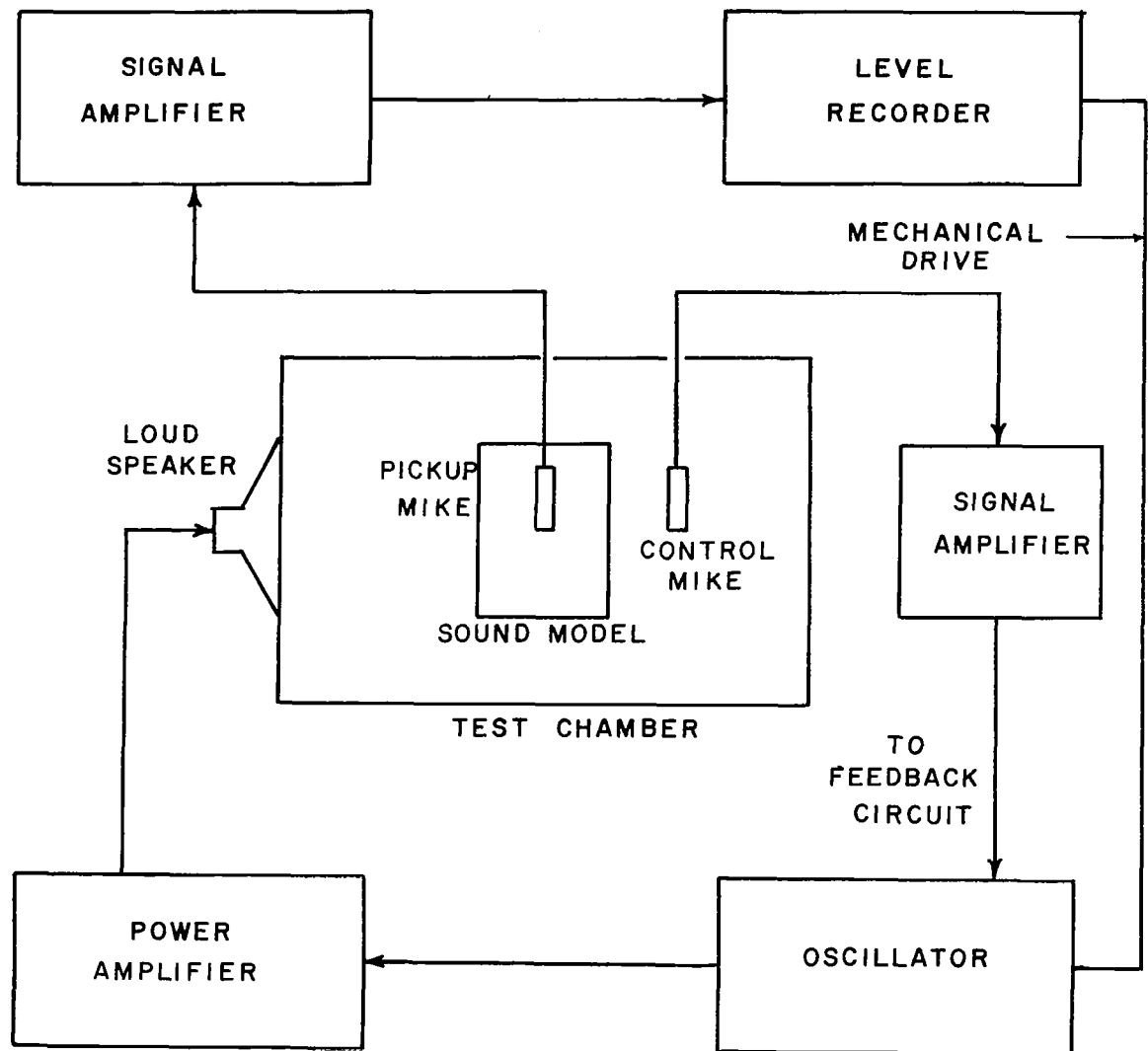


**FIGURE 21. EXPERIMENTAL ARRANGEMENT**

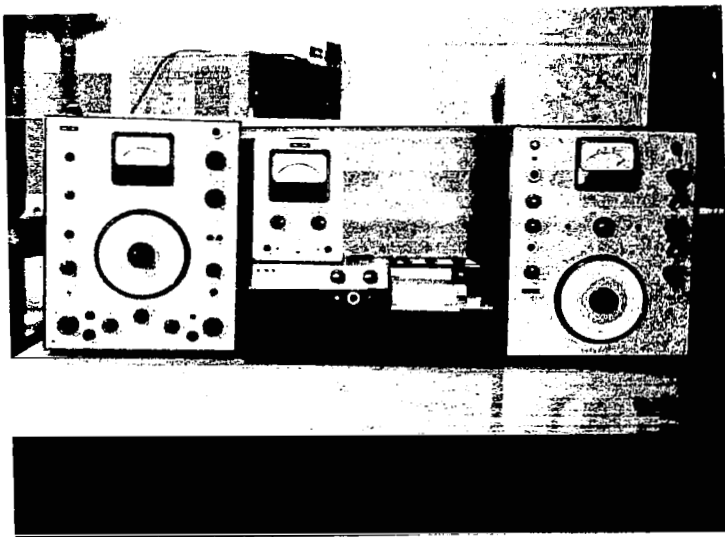


**FIGURE 22. ARRANGEMENT OF INSTRUMENTATION**

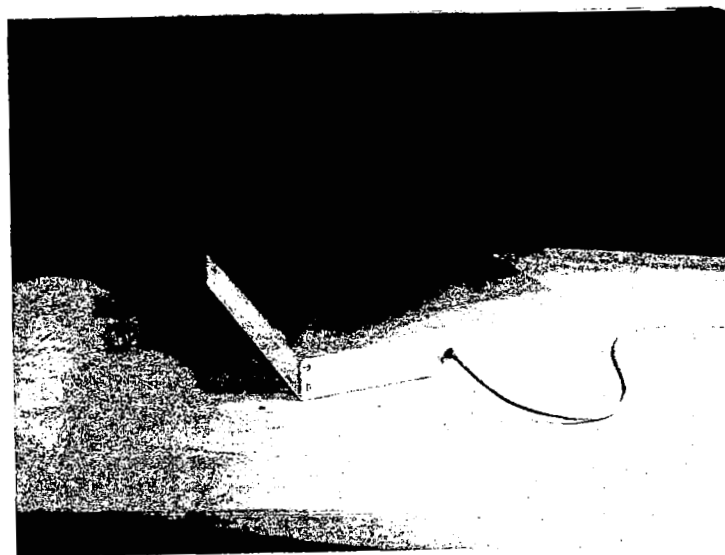


FIGURE 23. SOUND MODEL

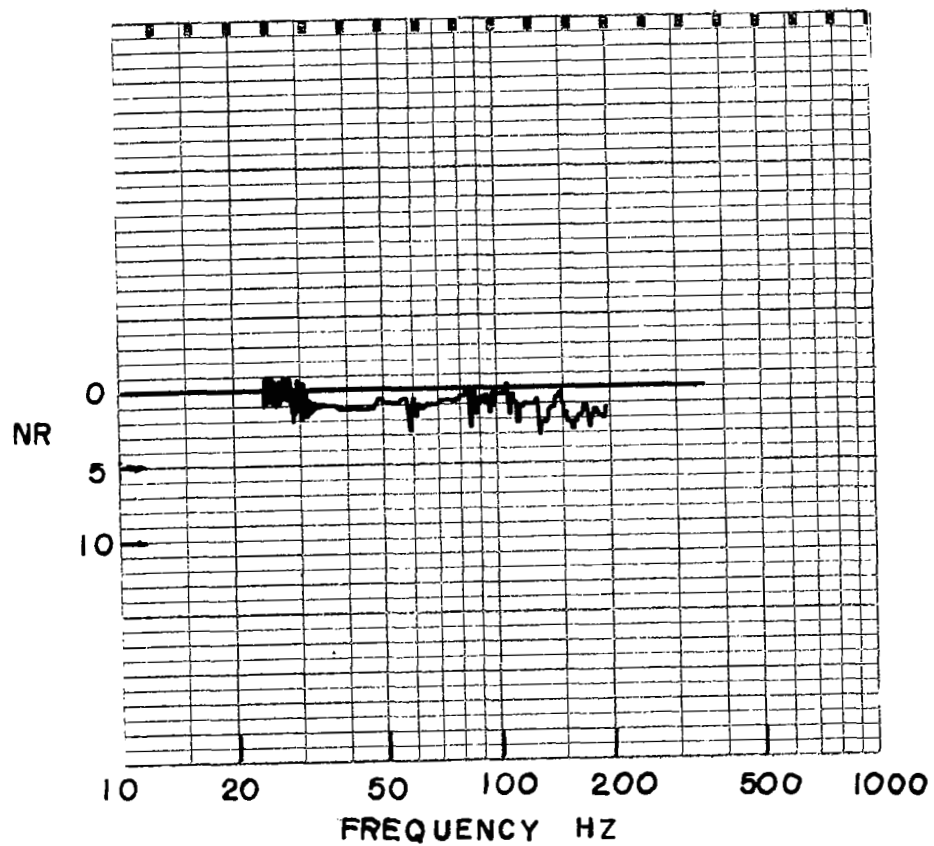


FIGURE 24. EXPERIMENTAL NOISE REDUCTION

.005 in. thickness aluminum was epoxied over this enclosure and the noise reduction of the enclosure was measured with the experimental setup of Figure 21. The results are shown in Figure 24 with the theoretical noise reduction which can be calculated from the given equations to be less than 1 dB. Thus, good agreement with theory is obtained.

Figure 25 shows the noise reduction of the same basic box with a .081 in. thickness test panel. Theoretical noise reduction can be calculated to be 9.6 and 12 dB for supported and clamped edges, respectively. The first resonance of the test panel is approximately 55 Hz if the edges are assumed to be free and approximately 138 Hz if clamped edges are assumed. These resonances are evident in the experimental results which show a marked decrease in noise reduction at 48 Hz and an actual amplification of sound pressure at 150 Hz.

A cylindrical enclosure is shown in Figure 26. The end plates are  $7\frac{1}{2}$  in. in diameter and are made of  $\frac{1}{2}$  in. thickness aluminum. The  $8\frac{1}{2}$  in. cylindrical test panel is of .005 in. thickness aluminum with a  $\frac{1}{8}$  in. overlap epoxied joint. The edges are also epoxied to the end plates. Experimental noise reduction is shown with the theoretical in Figure 27. Since  $\beta_1$  is greater than 20, the theoretical noise reduction of approximately 55 dB can be determined from the curve shown in Figure 19. Experimental noise reduction is seen to increase from 46 to 62 dB as the frequency changes from 20 to 200 Hz. However, these results agree with the theory as well as can be expected since the theoretical curve is independent of boundary conditions and does not consider the joint.

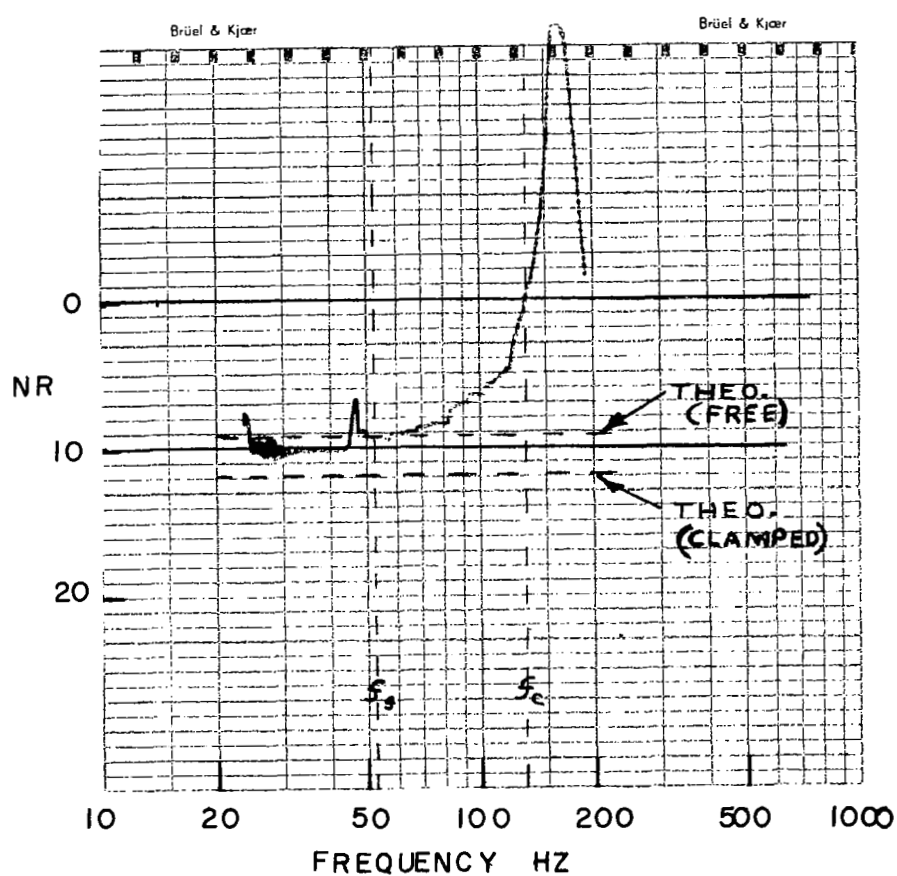


FIGURE 25. EXPERIMENTAL NOISE REDUCTION

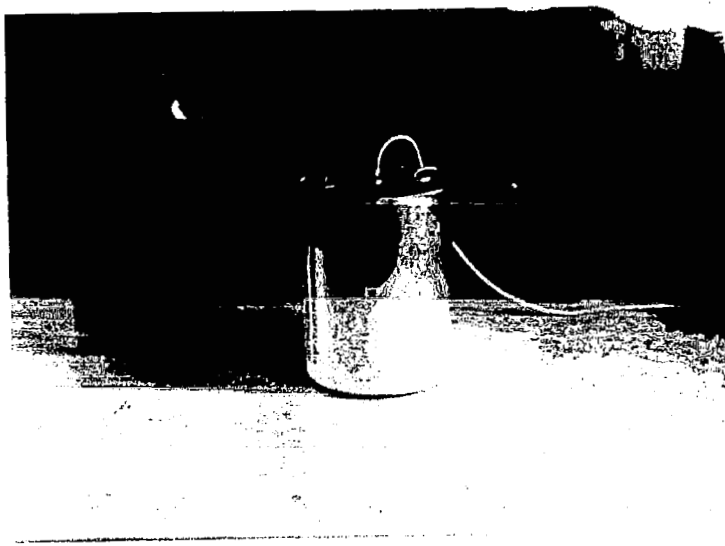


FIGURE 26. SOUND MODEL

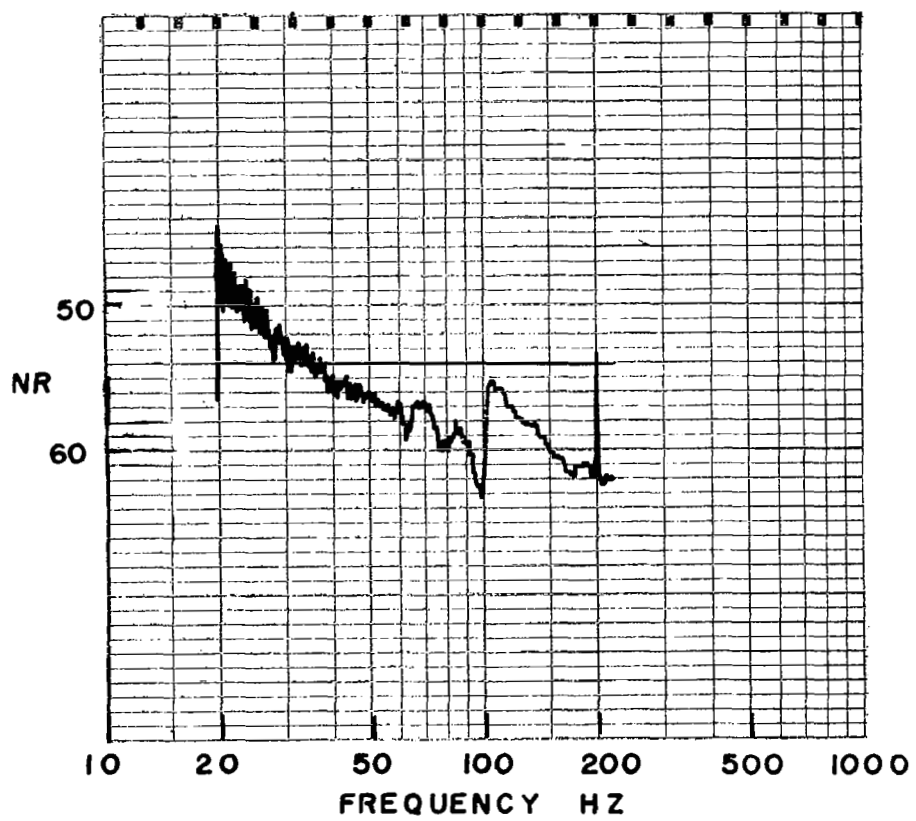


FIGURE 27. EXPERIMENTAL NOISE REDUCTION

A 9 in. steel sphere with  $1/64$  in. wall thickness is shown in Figure 28. Experimental and theoretical noise reduction are shown in Figure 29. The theoretical noise reduction can be determined from Figure 20 to be approximately 65 dB. The experimental noise reduction increases from 68 to 73 dB as the frequency sweeps from 25 to 200 Hz so that good agreement with theory is again obtained.

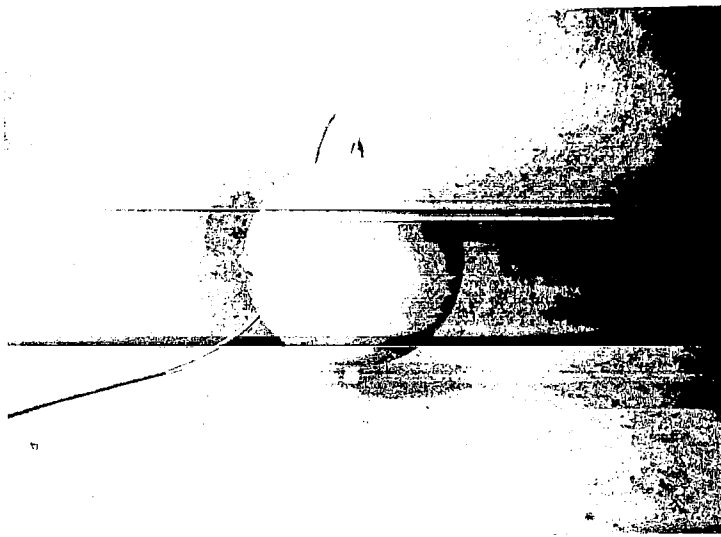


FIGURE 28. SOUND MODEL

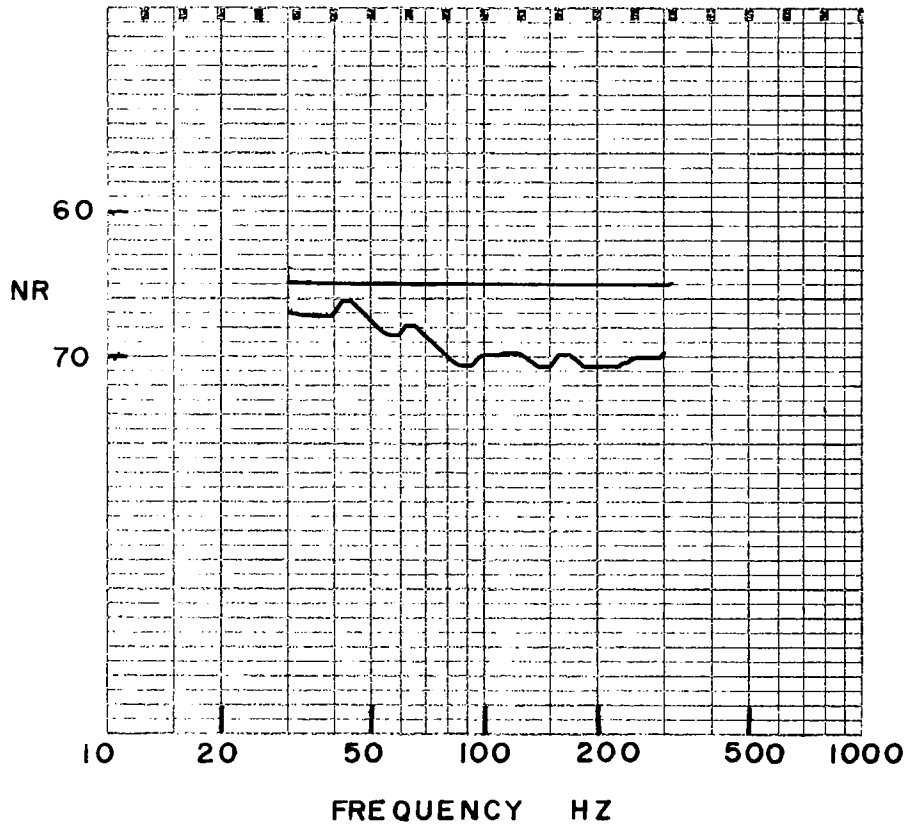


FIGURE 29. EXPERIMENTAL NOISE REDUCTION

## SUMMARY AND CONCLUSIONS

It has been shown that the geometric shape of a flexible panel exposed to a sound field can have a very significant effect on the panel's noise reduction. Rectangular and circular flat panels which have compliances that are flexure-controlled are seen to be much less resistant to volume displacements than membrane-controlled cylindrical and spherical panels. This indicates that structures designed for low-frequency noise reduction should avoid large, flat panels.

In general, it can be concluded that low-frequency noise reduction is independent of frequency. The compliance analysis presented in this paper is very similar to that required for pressure vessel design. However, acoustic and structural resonances must be considered in noise reduction analysis.

The design charts shown in Figures 7 through 20 can be used to predict the low-frequency noise reduction of structures. However, these curves are applicable only for panels whose dimensions are of the same order as the acoustic wavelength in the surrounding medium. Also, the structures must be below the first acoustic and structural resonances.

In the experimental investigation, the first rectangular enclosure and the cylindrical enclosure have equal volumes, flexible area, and panel thickness. However, the cylindrical enclosure is seen to have approximately 50 dB greater noise reduction than the rectangular enclosure. If .005 in. thickness end panels are used, the noise reduction of the cylindrical would drop to approximately 40 dB. A spherical

enclosure with the same volume and wall thickness can be shown to have approximately 50 dB noise reduction. This demonstrates well the conclusion that stiffer, membrane-controlled cylindrical and spherical enclosures have much greater noise reduction than enclosures having flexure-controlled flat panels.

#### LIST OF REFERENCES

- Beranek, L. L. 1960. Noise Reduction. McGraw-Hill Book Co., New York.
- Eichler, E. 1965. Thermal circuit approach to vibrations in coupled systems and the noise reduction of a rectangular box. J. Acoust. Soc. Am. 37:995-1007.
- Love, A. E. H. 1944. The Mathematical Theory of Elasticity. Dover Publications, Inc., New York, New York.
- Lyon, R. H. 1963. Noise reduction of rectangular enclosures with one flexible wall. J. Acoust. Soc. Am. 35:1791-1797.
- Lyon, R. H., Dietrich, C. W., Ungar, E. E., Pyle, R. W., Jr., Apfel, R. E. 1966. Low-frequency noise reduction of spacecraft structures. National Aeronautics and Space Administration, Washington, D. C., Report No. 1344.
- Timoshenko, S. 1959. Theory of Plates and Shells. McGraw-Hill Book Co., New York.
- White, P. H. 1960. Sound transmission through a finite, closed, cylindrical shell. J. Acoust. Soc. Am. 40:1124-1130.
- White, P. H. and Powell, A. 1966. A transmission of random sound and vibration through a rectangular double wall. J. Acoust. Soc. Am. 40:821-832.

## APPENDIX. LIST OF SYMBOLS

a	- cylinder radius
2a	- rectangular panel width
2b	- rectangular panel length
C	- speed of sound in air
$C_w$	- speed of sound in panel
$C_b$	- acoustic compliance
$C_p$	- panel compliance
D	- flexural rigidity - $Et^3/12(1-\sigma^2)$
E	- Young's modulus
f	- frequency
h	- wall thickness
$\ell$	- cylinder length
NR	- noise reduction
P	- external sound pressure
$P_b$	-internal sound pressure
r	- radius
t	- panel thickness
W	- normal deflection
X	- volume displacement
$\alpha$	- $B\ell/2$
$\beta$	- $\frac{Et}{4a^4 D}$
$\rho$	- density of air
$\pi$	- acoustic power
$\sigma$	- Poisson's ratio